OFDM Channel Estimation Based on Impulse Response Decimation: Analysis and Novel Algorithms

Stefano Rosati, *Member, IEEE*, Giovanni E. Corazza, *Senior Member, IEEE*, and Alessandro Vanelli-Coralli, *Senior Member, IEEE*

***Abstract*—In this paper, OFDM data-aided channel estimation based on the decimation of the Channel Impulse Response (CIR) through the selection of the Most Significant Samples (MSS) is addressed. Our aim is to approach the Minimum Mean Square Error (MMSE) channel estimation performance, while avoiding the need for a-priori knowledge of channel statistics (KCS). The optimal set of samples is defined in the instantaneous and average senses. We derive lower bounds on the estimation mean-square error (MSE) performance for any MSS selection strategy. We show how MSS-based channel estimation can approach these MSE lower bounds. We introduce novel MSS strategies oriented towards instantaneous decimation (Instantaneous Energy Selection - IES), and windowed decimation (Average Energy Selection - AES). We also consider decimation via Threshold Crossing Selection (TCS), which we characterize analytically, to derive the optimum threshold in the minimum MSE sense. We also propose a sub-optimal method for threshold setting that does not require KCS. Finally, we provide numerical results in terms of both MSE estimation performance and Bit Error Rate (BER) of a coded OFDM system using the proposed channel estimators, to show that they indeed approach MMSE performance.**

***Index Terms*—OFDM, channel estimation, minimum mean square error (MMSE), impulse response, pilot tone, DVB, threshold selection.**

I. Introduction

ORTHOGONAL Frequency Division Multiplexing (OFDM) [1] [2] has recently become the most attractive modulation scheme in broadband wireless systems for its flexibility and ability to cope with strongly dispersive channels using low-complexity equalizers, with a single tap per subcarrier. This is due to the fact that propagation channels which are frequency selective over the entire OFDM bandwidth may appear non-selective on each narrowband subcarrier. In particular, this is crucial for the case of OFDM single-frequency networks, where in order to achieve seamless radio coverage, identical signals are transmitted from widely separated sites. In this case, signal replicas may come with very large differential delays, giving rise to very sparse channel profiles.

Clearly, the equalizer will perform successfully if and only if accurate estimation of the Channel Transfer Function (CTF), or equivalently of the Channel Impulse Response (CIR), is performed at the receiver. In other words, channel estimation becomes *the* critical function which largely determines the overall receiver performance. For this reason, OFDM channel estimation is normally Data-Aided (DA) whereby known pilots are multiplexed into OFDM symbols, usually drawing a regular pattern of known subcarriers with constant inter-pilot frequency spacing. Using these pilots, channel estimation is performed in two steps: first, the CTF is punctually estimated on pilot subcarriers; then, channel estimates are interpolated over data subcarriers. These steps can be followed by averaging over several OFDM symbols, if useful.

In general, DA channel estimation methods differ in the way they interpolate or filter punctual DA Least Squares (DA-LS) channel estimates over data subcarriers. This can be accomplished using two-dimensional (2D) time-frequency Wiener Filtering (WF) [3], which is optimal in the Minimum Mean Square Error (MMSE) sense. Unfortunately, 2D-WF requires perfect knowledge of the channel statistics (KCS) and is burdened by large complexity. Complexity can be reduced if one abandons two-dimensional estimation in favor of a separate time and frequency approach. In [4], Hoeher et al. showed that by applying one-dimensional Wiener filters over time and frequency it is possible to reduce complexity and achieve good performance, if KCS is available. On the other hand, channel estimation can be accomplished by elaborating raw estimates in the time-domain using a Discrete Fourier Transform (DFT) based scheme. In [5], the MMSE channel estimator working in the time domain, which also requires complete KCS, has been proposed. In order to reduce computational complexity, using the singular value decomposition, several low-rank approximations to the MMSE estimator have been proposed in [6], [7]. On a more pragmatic basis, methods which require the minimum possible KCS and are applicable to any kind of Power Delay Profile (PDP) and in particular to sparse channels are appealing. In [8], Morelli and Mengali compared the MMSE approach with Maximum Likelihood (ML) channel estimation where complete KCS is not required, but only the PDP domain. This latter approach works well with dense multipath channels and quasi-uniform profiles. KCS

Paper approved by R. Schober, the Editor for Modulation and Signal Design of the IEEE Communications Society. Manuscript received October 7, 2009; revised April 30, 2010, April 8, 2011, and February 16, 2012.

S. Rosati was with DEIS/ARCES, University of Bologna, Italy. He is now with the Information Processing Group (IPG) and the Mobile Communications Laboratory (LCM), École Polytechnique Fédérale de Lausanne (EPFL), Switzerland (e-mail: stefano.rosati@epfl.ch).

G. E. Corazza and A. Vanelli-Coralli are with DEIS/ARCES, University of Bologna, Italy (e-mail: {giovanni.corazza, alessandro.vanelli}@unibo.it).

Digital Object Identifier 10.1109/TCOMM.2012.051012.090606

agnostic channel estimation can be achieved by interpolating the punctual DA-LS estimates using a DFT-based scheme without any elaboration in the time domain. Unfortunately, simplicity here goes along with mediocre performance [7], and much research work is being devoted to improving this approach without increasing complexity in any significant way.

The main idea to achieve this goal is the following: after the Inverse DFT (IDFT), not all the CIR samples are significant, because many may correspond to delays where no propagation channel paths are actually present. *Therefore, if one can devise a technique to decimate the CIR and retain only the significant samples, performance can be improved without complexity increase.* With this aim, Minn et al. [9] proposed to select only the J strongest samples, identified here as the Most Significant Samples (MSSs) of the CIR estimate, J being obviously a crucial design parameter. It is shown here that in the ideal case where J equals the actual number of non-zero channel taps, N_t, very good performance can be achieved; but when J differs from N_t, performance degrades rapidly. Instead of pre-determining a-priori the total MSS number, Kang et al. [10] proposed to select those samples for which the square module is above a threshold. We refer to this approach as Threshold Crossing Selection (TCS). In this way, a dynamic number of MSSs is selected per OFDM symbol. It is clear that the threshold value is critical to the algorithm performance. While in [10] the threshold was set according to heuristics, in [11] a genie-aided approach was followed, based again on ideal TCS.

The purpose of this paper is threefold. First, by defining the optimal set of selected samples, which minimizes the MSE, in both instantaneous and average senses, we derive lower bounds on the MSE performance for any MSS selection strategy. Comparing the obtained lower bounds with MMSE channel estimation performance, we conclude that MSS-based channel estimation has the potential to reach comparable performance with respect to the optimum MMSE approach, in particular when the number of pilots is significantly larger than the number of non-zero channel taps (as customary). Second, we analytically derive the optimum threshold value for TCS in the minimum MSE sense. We show that, by using the optimum threshold, TCS can tightly approach MMSE at high signal-to-noise ratio (SNR) values. Unfortunately, the optimal threshold depends on the actual channel PDP. For this reason, we propose a sub-optimal approach for threshold setting, which we show to yield comparable performance to the optimal threshold case with robustness against PDP variations. Third, we propose two novel MSS selection strategies, identified as Instantaneous Energy Selection (IES) and Average Energy Selection (AES), which do not require KCS, but only estimation of the received SNR. In particular, IES, as well as TCS, aims to decimate CIR estimate samples considering only their instantaneous energy, hence both IES and TCS are oriented towards instantaneous selection of MSSs. On the other hand, AES, which is oriented towards a windowed selection of MSSs, extends the observation window over several OFDM symbols, and, as a consequence of noise reduction, it closely approaches the MMSE performance, even for low SNR.

The remaining Sections are organized as follows. In Section II, the system model, the punctual DA estimation and the DFT interpolation, which are common to all proposed methods, are illustrated. The MSS MSE lower bounds are derived in Section III. In Section IV, TCS is discussed, in particular in IV-A the MSE analytical expression is derived, while the Sub-Optimal Threshold (SOT) method is proposed in Section IV-B. In Section V, the novel selection strategies, IES and AES, are presented. Numerical results are reported in Section VI; and, finally, conclusions are drawn in Section VII.

II. System Model and DA Channel Estimation

We consider an OFDM signal using N subcarriers, where the ℓ-th OFDM symbol, $\bar{s}_\ell = (s_{0,\ell}, \ldots, s_{N-1,\ell})$, is obtained as the N-point IDFT of the vector of complex symbols $\bar{x}_\ell = (x_{0,\ell}, \ldots, x_{N-1,\ell})$, as follows

$$s_{i,\ell} = \frac{1}{\sqrt{N}} \sum_{k=0}^{N-1} x_{k,\ell}\, \mathrm{e}^{\jmath\, 2\pi k i/N} \qquad i = 0, \ldots, N-1 \tag{1}$$

As discussed in the Introduction, the complex symbols $x_{k,\ell}$ carry either data information, $a_{k,\ell}$, or pilot reference symbols, $p_{k,\ell}$, used for DA channel estimation and synchronization. We assume to have uniformly scattered pilot tones in each OFDM symbol [1] (constant pilot frequency spacing), with periodic position shifts from symbol to symbol to improve coverage of the entire frequency comb [12]. Note that, to improve channel estimation performance, pilots can be transmitted with an energy boost factor β^2 with respect to data symbols (i.e. $E[p_{k,\ell}^2] = \beta^2 E_s$, where $E[a_{k,\ell}^2] = E_s$). Let $P(\ell)$ be the set of pilot subcarrier indices in the ℓ-th OFDM symbol, identified as *pilot pattern*, of size N_p. We can write

$$x_{k,\ell} = \begin{cases} p_{k,\ell} & \text{if } k \in P(\ell) \\ a_{k,\ell} & \text{if } k \notin P(\ell) \end{cases} \tag{2}$$

In order to avoid intersymbol interference and maintain subcarrier orthogonality even in multipath, a *cyclic prefix* of length N_g samples is inserted at the beginning of each OFDM symbol [13]. This is followed by digital to analog (D/A) conversion at sample rate $R = 1/T$, and using an appropriate analog transmission filter, $g_T(\tau)$, so that the time continuous signal can be written as

$$s(t) = \frac{1}{\sqrt{T_u}} \sum_{\ell=-\infty}^{\infty} \sum_{k=0}^{N-1} \mathrm{rect}\left(\frac{t}{T_S} - \frac{1}{2} - \ell\right) x_{k,\ell} \mathrm{e}^{\jmath\, 2\pi \frac{1}{T_u} k (t - T_g)} * g_T(\tau) \tag{3}$$

where $*$ denotes convolution, $\mathrm{rect}\,(t)$ represents the rectangular function[2], $T_u = NT$ and $T_g = N_g T$ represent respectively

[1] In many commercial OFDM systems, due to the insertion of null carriers at the edge of the OFDM spectrum, the assumption of uniformly scattered pilots does not hold strictly. However, it is worthwhile to use such an assumption (as also in [5]–[7], [9]–[11]) for two reasons: first, because it is the best pilot arrangement in terms of channel estimation minimum MSE for a given number of pilots and fixed energy [12]; second, because it allows a mathematical analysis which leads to algorithms which are proved by simulation to perform well even when the assumption does not hold strictly (i.e. considering the insertion of null carriers as guard bands). In fact in Section VI it is shown that, the proposed channel estimation schemes, which have been derived from a model assuming uniformly scattered pilot tones, perform well also considering commercial systems having non-uniformly scattered pilot tones.

[2] $\mathrm{rect}\,(t) = 1$ if $|t| \leq \frac{1}{2}, 0$ otherwise

the OFDM useful symbol duration, and the guard interval which is associated to the cyclic prefix. Therefore $T_S = T_u + T_g$ is the total OFDM symbol duration, and $f_u = 1/T_u$ is the subcarrier spacing. Notably, the normalization factor $\frac{1}{\sqrt{T_u}} = \frac{1}{\sqrt{N}} \cdot \frac{1}{\sqrt{T}}$ accounts for both the IDFT and the D/A normalization factors.

The OFDM signal is transmitted over a time-varying frequency selective fading channel, under the assumption that the channel coherence time exceeds T_S, which is necessary for correct OFDM operations. The baseband equivalent channel response can be modelled as a tapped delay line, while the received signal will be immersed in Additive White Gaussian Noise (AWGN). Assuming that the receiver filter $g_R(t)$ does not introduce linear distortion, and sampling the received signal every T seconds, yields

$$r(uT) = \sum_{i=0}^{L-1} h_i(uT)\, s(uT - iT) + n'(uT) \tag{4}$$

where $n'(uT)$ is the complex Gaussian noise sample with zero mean and N_0 variance, $h_i(t)$ represents the i-th channel tap complex gain, which comprises both channel propagation and filtering effects, and L is the length of the channel tapped delay line. In Rayleigh fading conditions, at any time instant $h_i(uT)$ can be modelled as a zero-mean complex Gaussian random variable. The total average channel energy is normalized to unity, i.e., $\sum_i E[h_i(uT)^2] = 1$. Removing the guard interval and re-arranging the vector at the input of the DFT, the samples belonging to the ℓ-th OFDM symbol can be collected into a vector $\bar{r}_\ell$ with components:

$$\begin{aligned} &r_{i,\ell} = r(((\ell-1)(N+N_g) + N_g + i)T) \\ &i = |u|_{N+N_g} - N_g \qquad \ell = \lceil u/(N+N_g) \rceil \end{aligned} \tag{5}$$

where $\lceil \cdot \rceil$ indicates the smallest integer larger than the argument. Having assumed that the maximum delay is smaller than the guard interval duration, (again, this is always verified in normal OFDM operation [14]), the observed samples at the output of the DFT are:

$$y_{k,\ell} = \frac{1}{\sqrt{N}} \sum_{i=0}^{N-1} r_{i,\ell}\, \mathrm{e}^{-\jmath 2\pi k i/N} = x_{k,\ell} H_{k,\ell} + n_{k,\ell} \tag{6}$$

$$k = 0, \ldots, N-1 \tag{7}$$

where $n_{k,\ell}$ is the complex AWGN sample in the frequency domain, which still has zero-mean and variance N_0, and $H_{k,\ell}$ is the CTF sample at the k-th subcarrier, in the ℓ-th symbol. The latter can be expressed as:

$$H_{k,\ell} = \sum_{i=0}^{L-1} h_{i,\ell}\, \mathrm{e}^{-\jmath 2\pi k i/N} \qquad k = 0, \ldots, N-1 \tag{8}$$

Since we have assumed that the channel coherence time exceeds T_S, the channel taps remain constant over an entire OFDM symbol duration, thus we define $h_{i,\ell} = h_i(\ell T_S)$ as the complex gain of the i-th channel tap during the ℓ-th OFDM symbol. The collection of the channel taps is identified as the Channel Impulse Response (CIR), having length L, but containing only N_t non-zero channel taps. As a consequence of filtering, propagation paths energy will be spread over several channel taps, which are therefore correlated. In the following, we will introduce the assumption of uncorrelated channel taps as a working hypothesis to derive the TCS SOT algorithm, and we will drop the assumption in the numerical results Section, to prove functionality under realistic conditions.

Considering a generic pilot tone positioned at the k-th subcarrier in the ℓ-th OFDM symbol, the punctual LS estimate is given by:

$$\hat{H}^{LS}_{k,\ell} = \frac{y_{k,\ell}}{p_{k,\ell}} = H_{k,\ell} + \frac{n_{k,\ell}}{p_{k,\ell}} \qquad k \in P(\ell) \tag{9}$$

As discussed previously, DA channel estimation methods differ in the way they interpolate the punctual observations, $\hat{H}^{LS}_{k,\ell}$, over data subcarriers. We consider here the DFT interpolation approach, which would be optimal in the absence of noise and with sufficient pilot density[3]. Under the assumption that pilot symbols are present in all OFDM symbols, time interpolation is not strictly necessary, but it can always be added if useful. Here we focus on the always necessary frequency-domain interpolation, which is performed in three steps. First, an IDFT is applied to the vector of punctual estimates to produce a CIR estimate sample, $\hat{h}_{i,\ell}$, as follows

$$\hat{h}_{i,\ell} = \frac{1}{N_p} \sum_{k'=0}^{N_p-1} \hat{H}^{LS}_{k(k'),\ell}\, \mathrm{e}^{-\jmath 2\pi k' i/N_p} \quad i = 0, \ldots, N_p - 1 \tag{10}$$

where $k(k')$ is an indexing function which points to the N_p positions of the scattered pilots within the OFDM symbol. This function has been introduced to point out the fact that only the N_p CTF estimates are considered in the sum. Then, assuming that $N_p > L$, CTF estimation over the entire frequency comb can be obtained by zero padding the CIR over the entire OFDM symbol duration:

$$\hat{\bar{h}}^{ZP}_{\ell} = \{\underbrace{\hat{h}_{0,\ell}, \ldots, \hat{h}_{N_p-1,\ell}}_{N_p} \underbrace{0, \ldots, 0}_{N-N_p}\} \tag{11}$$

and finally by applying a DFT:

$$\hat{\bar{H}}^{LS}_{\ell} = DFT\{\hat{\bar{h}}^{ZP}_{\ell}\} \tag{12}$$

As will be shown in the following, it is possible to compute the MSE associated to this DA estimation/DTF interpolation method in closed form. More importantly, it is possible to improve the resulting MSE by adopting a suitable sample selection strategy.

III. Most Significant Samples Selection: MSE Lower Bound

As anticipated in the Introduction, not all CIR estimate samples are significant; in fact, many samples may correspond to delays where no channel taps are actually present, and consequently they only contain noise. Therefore, it is possible to reduce drastically the noise presence, especially when the

[3]As consequence of the Nyquist-Shannon sampling theorem, in the absence of noise and with sufficient pilot density, the DFT interpolation exactly reconstructs the vector $H_{k,\ell}$.

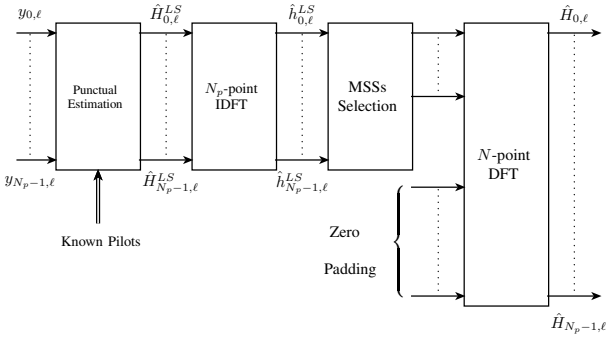

Fig. 1. Block diagram of Channel Estimator based on Most Significant Sample selection.

CIR is very sparse, by decimating the impulse response into the subset $\mathcal{S}(\ell)$ of *most significant samples* after the IDFT:

$$\hat{h}^{MSS}_{i,\ell} = \begin{cases} \hat{h}_{i,\ell} & \text{if } i \in \mathcal{S}(\ell) \\ 0 & \text{if } i \notin \mathcal{S}(\ell) \end{cases} \tag{13}$$

The complete block diagram is shown in Fig. 1. Obviously, the critical aspect of this method is the strategy used in forming $\mathcal{S}(\ell)$, upon which the MSE is completely dependent. It is both interesting and essential to obtain a lower bound on the MSE for DA channel estimation based on MSS selection. The first step towards the achievement of this goal is to model statistically the CIR estimate samples, $\hat{h}_{i,\ell}$. Substituting (9) in (10), we obtain

$$\hat{h}_{i,\ell} = \frac{1}{N_p}\left(\sum_{k'=0}^{N_p-1} H_{k(k'),\ell}\, \mathrm{e}^{-\jmath\, 2\pi k' i/N_p} + \right. \\ \left. + \sum_{k'=0}^{N_p-1} \frac{n_{k(k'),\ell}}{p_{k(k'),\ell}} \mathrm{e}^{-\jmath\, 2\pi k' i/N_p}\right) \quad i = 0, \ldots, N_p-1 \tag{14}$$

Thus, we can write the CIR estimate as the sum of the correct value, $h_{i,\ell}$, and a noise component, $\nu_{i,\ell}$:

$$\hat{h}_{i,\ell} = h_{i,\ell} + \nu_{i,\ell} \tag{15}$$

where:

$$\nu_{i,\ell} = \frac{1}{N_p} \sum_{k'=0}^{N_p-1} \frac{n_{k(k'),\ell}}{p_{k(k'),\ell}} \mathrm{e}^{-\jmath\, 2\pi k' i/N_p} \tag{16}$$

Due to the statistical independence of the $n_{k,\ell}$ samples, the noise components are distributed as zero-mean complex Gaussian random variables with variance $1/\rho N_p$:

$$\nu_{i,\ell} \sim \mathcal{N}_c\left(0, \frac{1}{\rho N_p}\right) \tag{17}$$

where $\rho = \beta^2 E_s/N_0$ represents the pilot energy to noise ratio, and $\mathcal{N}_c\left(\mu, \sigma^2\right)$ represents the probability density function of a complex Gaussian random variable with mean μ and variance σ^2. Therefore, the CIR estimate samples, $\hat{h}_{i,\ell}$, are also complex Gaussian random variables distributed as:

$$\hat{h}_{i,\ell} \sim \begin{cases} \mathcal{N}_c\left(0, \frac{1}{\rho N_p} + \gamma_i^2\right) & \text{if } i \in \mathcal{C} \\ \mathcal{N}_c\left(0, \frac{1}{\rho N_p}\right) & \text{if } i \notin \mathcal{C} \end{cases} \quad i = 0, \ldots, N_p-1 \tag{18}$$

where γ_i^2 represents the average energy of the i-th channel tap and $\mathcal{C}$ is the set of indices corresponding to the N_t samples where the channel tap energy is greater than zero, i.e. $i \in \mathcal{C}$ iff $\gamma_{\mathrm{i}}^2 \neq 0$.

In selecting or rejecting any CIR estimate sample, four events are possible:

Noise Excision (NE): A CIR estimate sample, corresponding to a delay where no channel tap energy is present, is correctly rejected. This corresponds to the very reason at the heart of MSS, and occurs with probability P^{NE}.

Noise Holding (NH): A CIR estimate sample, corresponding to a delay where no channel tap energy is present, is reckoned as significant. This case contributes to the MSE with the noise component contained in the CIR estimate, and occurs with probability $P^{\mathrm{NH}} = 1 - P^{\mathrm{NE}}$.

Tap Excision (TE): A CIR estimate sample, corresponding to a delay where channel tap energy is present, is rejected. This case contributes to the MSE with the neglected tap energy, and occurs with probability P^{TE}.

Tap Holding (TH): A CIR estimate sample, corresponding to a delay where channel tap energy is present, is reckoned as significant. This case contributes to the MSE with the noise component contained in the CIR estimate, and occurs with probability $P^{\mathrm{TH}} = 1 - P^{\mathrm{TE}}$.

Considering (13) and (15), the estimation square errors $|\varepsilon_{i,\ell}|^2 = |h_{i,\ell} - \hat{h}^{MSS}_{i,\ell}|^2$ corresponding to the four events are given by:

$$|\varepsilon_{i,\ell}|^2 = \begin{cases} 0 & \text{if } i \notin \mathcal{C} \wedge i \notin \mathcal{S}(\ell) \quad \text{Noise Excision} \\ |\nu_{i,\ell}|^2 & \text{if } i \notin \mathcal{C} \wedge i \in \mathcal{S}(\ell) \quad \text{Noise Holding} \\ |h_{i,\ell}|^2 & \text{if } i \in \mathcal{C} \wedge i \notin \mathcal{S}(\ell) \quad \text{Tap Excision} \\ |\nu_{i,\ell}|^2 & \text{if } i \in \mathcal{C} \wedge i \in \mathcal{S}(\ell) \quad \text{Tap Holding} \end{cases} \tag{19}$$

The overall Square Error (SE) for the ℓ-th OFDM symbol can therefore be written as the sum of three contributions from, respectively, noise holding, tap excision, and tap holding:

$$\mathrm{SE}(\ell) = \sum_{i=0}^{N_p-1} |\varepsilon_{i,\ell}|^2 = \sum_{i \in \mathcal{S}(\ell)\setminus\mathcal{C}} |\nu_{i,\ell}|^2 + \\ + \sum_{i \in \mathcal{C}\setminus\mathcal{S}(\ell)} |h_{i,\ell}|^2 + \sum_{i \in \mathcal{S}(\ell)\cap\mathcal{C}} |\nu_{i,\ell}|^2 \tag{20}$$

where $B \setminus A$ represents the relative complement of A in B (i.e. $B \setminus A = \{x \in B \,|\, x \notin A\}$). Now we want define the optimal set of samples, $S_{opt}(\ell)$, which minimizes the SE of the ℓ-th OFDM symbol, $\mathrm{SE}(\ell)$. Note that, if $\mathcal{S}(\ell)$ is a subset of $\mathcal{C}$, $\mathcal{S}(\ell) \subseteq \mathcal{C}$, then NH is always avoided. However, the latter is necessary but not sufficient for the optimality of $\mathcal{S}(\ell)$ in the minimum SE sense. In fact, it is interesting to note that $S_{opt}(\ell)$ can be strictly smaller than $\mathcal{C}$. Intuitively, if a sample contains an actual CIR tap, but this is overcome by noise, it pays off to decimated it out of the estimation comb. The necessary and sufficient condition on the optimality of $\mathcal{S}(\ell)$ is that $i \in \mathcal{S}(\ell)$ iff $|h_{i,\ell}|^2 > |\nu_{i,\ell}|^2$, therefore

$$\mathcal{S}_{opt}(\ell) \equiv \left\{i : |h_{i,\ell}|^2 > |\nu_{i,\ell}|^2,\ i = 0, \ldots, N_p-1\right\} \tag{21}$$

Proof: $\mathrm{SE}(\ell)$ is the sum of N_p non-negative terms, $\mathrm{SE}(\ell) = \sum_{i=0}^{N_p-1} |\varepsilon_{i,\ell}|^2$. For each i we can actually have two

cases, obtained by grouping holding and excision[4] events:

$$|\varepsilon_{i,\ell}|^2 = \begin{cases} |\nu_{i,\ell}|^2 & \text{if } i \in \mathcal{S}(\ell) \text{ Holding} \\ |h_{i,\ell}|^2 & \text{if } i \notin \mathcal{S}(\ell) \text{ Excision} \end{cases} \quad \forall\, i = 0, \ldots, N_p - 1 \tag{22}$$

Therefore, the minimum $\mathrm{SE}(\ell)$ is obtained by minimizing each term of the above sum separately:

$$\mathrm{SE}_{min}(\ell) = \min \mathrm{SE}(\ell) = \sum_{i=0}^{N_p-1} \min\left\{|\nu_{i,\ell}|^2, |h_{i,\ell}|^2\right\} \tag{23}$$

Hence, if and only if $|h_{i,\ell}|^2 > |\nu_{i,\ell}|^2$ for all $i \in \mathcal{S}(\ell)$, and $|h_{i,\ell}|^2 < |\nu_{i,\ell}|^2$ for all $i \notin \mathcal{S}(\ell)$, then $\mathrm{SE}(\ell) = \mathrm{SE}_{min}(\ell)$. Considering that both $|h_{i,\ell}|^2$ and $|\nu_{i,\ell}|^2$ are continuous random variables, and thus, the probability to have $|h_{i,\ell}|^2 = |\nu_{i,\ell}|^2$ is null, the above conditions can be can expressed as in (21). ■

Although it is clear that only a genie-aided receiver could find the $S_{opt}(\ell)$ as defined above, this is still a very useful objective even for practical receivers, as discussed in Sections IV and V. Here, it is important to derive the performance limits that correspond to the use of $S_{opt}(\ell)$. In this case, the SE for the ℓ-th OFDM symbol reduces to

$$\mathrm{SE}_{min}(\ell) = \sum_{i \in \mathcal{C} \setminus \mathcal{S}_{opt}(\ell)} |h_{i,\ell}|^2 + \sum_{i \in \mathcal{S}_{opt}(\ell)} |\nu_{i,\ell}|^2 \tag{24}$$

By averaging over the channel and noise statistics, it can be shown that the resulting lower bound on MSE, achievable by using instantaneously the optimum set of samples $S_{opt}(\ell)$, and identified as $\mathrm{MSE}(opt)$, is given by:

$$\mathrm{MSE}(opt) = E[\mathrm{SE}_{min}(\ell)] = \sum_{i \in \mathcal{C}} \frac{\gamma_i^2}{1 + \rho N_p \gamma_i^2} \tag{25}$$

The analytical derivation is provided in Appendix A. It is very interesting to note that the result coincides with the MMSE expression derived in [7], [8].

It is hard to presume a-priori that the average performance associated to instantaneous optimal selection, $\mathrm{MSE}(opt)$, corresponds to the MMSE, since they come from very different assumptions: the MMSE approach requires ideal KCS, while the instantaneous optimal selection requires the knowledge on the specific realizations of the channel response and thermal noise. This does not mean that $\mathrm{MSE}(opt)$ requires complete knowledge of the channel and the noise realizations, which could lead to infer that $\mathrm{MSE}(opt) < \mathrm{MMSE}$. Indeed, instantaneous optimal selection needs just a minimum information (a binary information) on the specific realizations. It is sufficient to know whether $|h_{i,\ell}|$ is greater or smaller than $|\nu_{i,\ell}|$. On the contrary, the MMSE approach requires full and ideal KCS.

However, since finding the exact $\mathcal{S}_{opt}(\ell)$ requires aid from a genie, we investigate also an alternative approach. The idea is to make decisions based on average rather than instantaneous quantities, the advantage being that estimation becomes possible. Assuming wide-sense stationarity, which eliminates the dependence on ℓ, we define the optimal set in the average sense, $\mathcal{S}_{avg}$, as:

$$\mathcal{S}_{avg} \equiv \left\{i : E\left[|h_i|^2\right] > E\left[|\nu_i|^2\right],\ i = 0, \ldots, N_p - 1\right\} \tag{26}$$

[4]Note that in case $i \notin \mathcal{C}$ it holds $|h_{i,\ell}|^2 = 0$

The above is general and can be applied to any channel conditions. Specifying it for our channel model, it becomes

$$i \in \mathcal{S}_{avg} \Longleftrightarrow \gamma_i^2 > \frac{1}{\rho N_p} \tag{27}$$

Therefore, the $\mathrm{MSE}(avg)$, corresponding to the use of $\mathcal{S}_{avg}$ can be written as:

$$\mathrm{MSE}(avg) = \sum_{i \in \mathcal{C} \setminus \mathcal{S}_{avg}} E\left[|h_i|^2\right] + \sum_{i \in \mathcal{S}_{avg}} E\left[|\nu_i|^2\right] = \tag{28}$$

$$= \sum_{i \in \mathcal{C} \setminus \mathcal{S}_{avg}} \gamma_i^2 + \sum_{i \in \mathcal{S}_{avg}} \frac{1}{\rho N_p} \tag{29}$$

As a particular case, when ρN_p is large enough to ensure that $(\rho N_p)^{-1} < \gamma_i^2$, $\forall i \in \mathcal{C}$, then $\mathcal{S}_{avg} \equiv \mathcal{C}$, and it holds:

$$\mathrm{MSE}(avg) = \sum_{i \in \mathcal{C}} E\left[|\nu_i|^2\right] = \frac{N_t}{\rho N_p} \tag{30}$$

It is interesting to compare the $\mathrm{MSE}(avg)$ to LS and MMSE performance. Following lines similar to [7], the MSE expression for LS, $\mathrm{MSE}(LS)$, is given by:

$$\mathrm{MSE}(LS) = \sum_{i=0}^{N_p-1} E\left[|h_i - \hat{h}_i|^2\right] = \sum_{i=0}^{N_p-1} E\left[|\nu_i|^2\right] = \frac{1}{\rho} \tag{31}$$

We observe that, for $\mathcal{S}_{avg} \equiv \mathcal{C}$, $\mathrm{MSE}(avg)$ improves over $\mathrm{MSE}(LS)$ by a factor equal to $\frac{N_t}{N_p} < 1$. In practice, N_t is much smaller than N_p, yielding a much lower MSE value. Regarding MMSE estimation, as anticipated previously, under the assumption of uniformly scattered pilots the MMSE is given by:

$$\mathrm{MMSE} = \sum_{i \in \mathcal{C}} \frac{\gamma_i^2}{1 + \rho N_p \gamma_i^2} \tag{32}$$

Assuming a uniform power delay profile, where all the N_t taps have equal energy:

$$\gamma_i^2 = \begin{cases} \frac{1}{N_t} & i \in \mathcal{C} \\ 0 & i \notin \mathcal{C} \end{cases} \tag{33}$$

the MMSE becomes:

$$\mathrm{MMSE} = \frac{1}{1 + \frac{\rho N_p}{N_t}} = \frac{1}{1 + \frac{1}{\mathrm{MSE}(avg)}} \tag{34}$$

We observe that $\lim_{\frac{\rho N_p}{N_t} \to \infty} \mathrm{MMSE} = \mathrm{MSE}(avg)$, which confirms that *the average approach is asymptotically optimum*. In practice, $\mathrm{MSE}(avg)$ approaches MMSE performance rapidly. As an example, Fig. 2 shows the ratio between $\mathrm{MSE}(avg)$ and MMSE in the case of uniform power delay profile, for several values of SNR, and of the ratio between number of pilots over number of taps. In the end, *MMSE is the ultimate performance limit for both instantaneous and average strategies*.

Our purpose is now to investigate selection strategies which can nearly achieve the MMSE performance without KCS. As anticipated in the Introduction, in this paper we deal with three different strategies: Threshold Crossing Selection (TCS), Instantaneous Energy Selection (IES), and Average Energy Selection (AES). TCS and IES, which decimate CIR samples

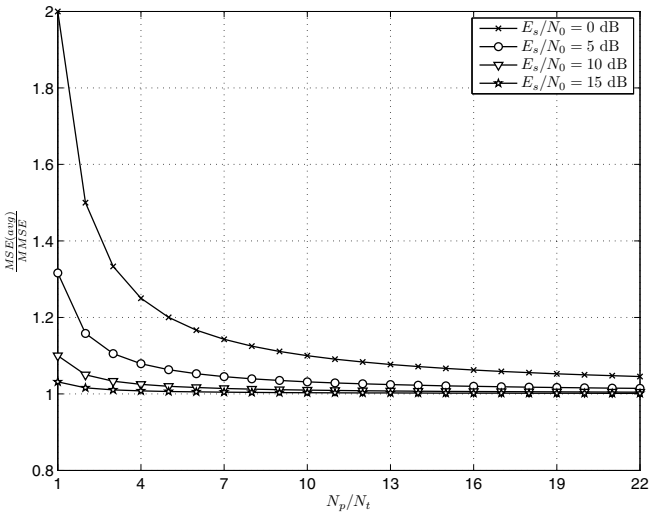

Fig. 2. $\mathrm{MSE}(avg)$ normalized to the MMSE as a function of the ratio between number of pilots over number of taps, for several values of SNR. Using uniform channel and $\beta^2 = 1$.

without using memory from previous OFDM symbols, are oriented towards the use of $S_{opt}(\ell)$. On the other hand, AES, which decimates CIR samples by extending the observation window over several OFDM symbols, is oriented towards the use of S_{avg}.

IV. Threshold Crossing Selection

The TCS strategy for identifying the MSS set, which has been treated in [9], [10], [11], [15], [16], is based on the concept that only those samples which overcome a threshold ξ in absolute value are retained:

$$\mathcal{S}_{\mathrm{TCS}}(\ell) \equiv \left\{ i : |\hat{h}_{i,\ell}| > \xi,\ i = 0, \ldots, N_p - 1 \right\} \tag{35}$$

In [10, eq. (21)] the threshold ξ has been empirically set equal to the square root of twice the noise level (which should be estimated):

$$\xi = \sqrt{\frac{2}{\rho N_p}} \tag{36}$$

In [11, eq. (6)], a criterion is proposed for establishing a set of threshold values that requires the knowledge of the entire CIR power profile:

$$\xi_i = \sqrt{\frac{1}{\rho N_p} \ln\left(2 + \rho N_p \gamma_i^2\right)} \qquad i = 0, \ldots, N_p - 1 \tag{37}$$

In [15] we proposed a pragmatic approach to set the threshold without KCS, based on a specification for the overall NH probability:

$$\xi = \sqrt{\frac{\ln\left(N_p / \overline{P^{\mathrm{ONH}}}\right)}{\rho N_p}} \tag{38}$$

where $\overline{P^{\mathrm{ONH}}}$ is a design parameter. In [16] the same threshold setting has been applied to OFDM time-frequency synchronization problems.

These methods are reasonable but based on heuristics. Here, we find the optimal threshold by deriving the closed form expression for the TCS MSE performance, and then by minimizing it with respect to ξ.

A. TCS MSE: Analytical Expression

Adopting TCS with a threshold ξ, and considering (18) and (35), we can write the TH probability in the i-th sample, as:

$$P_i^{\mathrm{TH}} = \mathrm{Prob}\left[|\hat{h}_i| > \xi \,\middle|\, i \in \mathcal{C} \right] = \mathrm{e}^{-\frac{\rho N_p \xi^2}{1+\gamma_i^2 \rho N_p}} \quad \forall\, i \in \mathcal{C} \tag{39}$$

Similarly, the NH probability is given by:

$$P_i^{\mathrm{NH}} = \mathrm{Prob}\left[|\hat{h}_i| > \xi \,\middle|\, i \notin \mathcal{C} \right] = \mathrm{e}^{-\rho N_p \xi^2} \quad \forall\, i \notin \mathcal{C} \tag{40}$$

Notably the NH probability does not depend on i, hence we will refer to it as P^{NH}. In summary, adopting TCS, the MSE can be found to be [15]:

$$\begin{aligned}
\mathrm{MSE}^{\mathrm{TCS}} &= \sum_{i=0}^{N_p-1} E\left[|\varepsilon_i|^2\right] = \\
&= \sum_{i \in \mathcal{C}} \left(P_i^{\mathrm{TH}} E\left[|\nu_i|^2 | \mathrm{TH}\right] + P_i^{\mathrm{TE}} E\left[|h_i|^2 | \mathrm{TE}\right] \right) + \\
&\quad + \sum_{i \notin \mathcal{C}} P^{\mathrm{NH}} E\left[|\nu_i|^2 | \mathrm{NH}\right] = \\
&= \sum_{i \in \mathcal{C}} \left[\frac{\mathrm{e}^{-\frac{\rho N_p \xi^2}{1+\gamma_i^2 \rho N_p}}}{\rho N_p} + \left(1 - e^{-\frac{\rho N_p \xi^2}{1+\gamma_i^2 \rho N_p}}\right) \right. \\
&\quad \left. \left(\gamma_i^2 - \frac{\xi^2}{e^{\xi^2/\gamma_i^2} - 1}\right) \right] + \\
&\quad + (N_p - N_t) \frac{\mathrm{e}^{-\rho N_p \xi^2} \left(1 + \rho N_p \xi^2\right)}{\rho N_p}
\end{aligned} \tag{41}$$

Our aim here is to derive analytically the optimal threshold ξ_{opt} which minimizes the MSE:

$$\xi_{opt} = \arg \min_{\xi} \mathrm{MSE}^{\mathrm{TCS}}(\xi) \tag{42}$$

A necessary condition is obtained by setting the first derivative of (41) to zero:

$$\begin{aligned}
&\sum_{i \in \mathcal{C}} 2\xi \left\{ \frac{e^{-\frac{\rho N_p \xi^2}{1+\gamma_i^2 \rho N_p}}}{1 + \gamma_i^2 \rho N_p} \left[\rho N_p \left(\gamma_i^2 - \frac{\xi^2}{e^{\frac{\xi^2}{\gamma_i^2}} - 1} \right) - 1 \right] + \right. \\
&\left. + \frac{1 + e^{\frac{\xi^2}{\gamma_i^2}} \left(\frac{\xi^2}{\gamma_i^2} - 1 \right)}{\left(e^{\frac{\xi^2}{\gamma_i^2}} - 1 \right)^2} \left(1 - e^{-\frac{\rho N_p \xi^2}{1+\gamma_i^2 \rho N_p}} \right) \right\} + \\
&- 2\rho N_p \xi^3 \mathrm{e}^{-\rho N_p \xi^2} (N_p - N_t) = 0
\end{aligned} \tag{43}$$

Equation (43) is in an implicit form, and can only be solved numerically, with knowledge of the channel tap power profile γ_i^2, $i \in \mathcal{C}$, and pilot energy to noise ratio ρ. We therefore proceed as follows.

B. Sub-Optimal Threshold (SOT)

In order to achieve an explicit solution, as well as to avoid the required KCS, let's introduce a few assumptions and

approximations. First, we assume a uniform channel tap power profile as in (33), so that (43) becomes:

$$2N_t\xi\left\{\frac{e^{-\frac{\rho N_t N_p\xi^2}{N_t+\rho N_p}}N_t}{N_t+\rho N_p}\left[\rho N_p\left(\frac{1}{N_t}-\frac{\xi^2}{\mathrm{e}^{N_t\xi^2}-1}\right)-1\right]+\right.$$
$$\left.+\frac{1+e^{N_t\xi^2}\left(N_t\xi^2-1\right)}{\left(e^{N_t\xi^2}-1\right)^2}\left(1-\mathrm{e}^{-\frac{\rho N_t N_p\xi^2}{N_t+\rho N_p}}\right)\right\}+$$
$$-2\rho N_p\xi^3\mathrm{e}^{-\rho N_p\xi^2}(N_p-N_t)=0 \tag{44}$$

Second, note that $N_t+\rho N_p \approx \rho N_p$, which is justified even in low SNR regions, since the number of pilots N_p is typically large enough to ensure that $\rho N_p >> N_t$. Using this approximation, after considerable algebra, we obtain:

$$\mathrm{e}^{(\rho N_p-N_t)\xi^2}=\frac{N_p-N_t}{\rho N_p\xi^2-1}\left(\frac{\rho N_p\xi}{N_t}\right)^2 \tag{45}$$

Finally, exploiting the fact that $\rho N_p\xi^2 >> 1$, we have

$$\frac{N_p-N_t}{\rho N_p\xi^2-1}\left(\frac{\rho N_p\xi}{N_t}\right)^2\approx\frac{(N_p-N_t)\rho N_p}{N_t^2} \tag{46}$$

and we can find the following explicit solution for the sub-optimal threshold:

$$\xi_{so}=\sqrt{\frac{\ln\left(\frac{(N_p-\hat{N}_t)\rho N_p}{\hat{N}_t^2}\right)}{\rho N_p-\hat{N}_t}} \tag{47}$$

where $\hat{N}_t$ is a parameter estimating the number of non-zero taps of the CIR. Of course, the best performance is obtained in case of $\hat{N}_t = N_t$, however, as shown in the numerical results, the SOT approach is robust even in the case of a mismatch between N_t and $\hat{N}_t$. Furthermore, the SOT values obtained using expression (47), and those obtained by solving numerically (44) are very close for all SNR values, and thus the approximations are justified and practically useful.

V. Energy-based MSS Selection Strategies

We now discuss two approaches based on received energy. The first, IES, pursues instantaneous decimation and therefore seeks to approach $S_{opt}(\ell)$. The second, AES, averages over a window of several OFDM symbols, and thus goes after S_{avg}. Neither of two methods require KCS, but only the estimation of the received SNR.

A. Instantaneous Energy Selection

The idea is to orderly select the strongest CIR estimate samples until the collected energy reaches the estimate of the total received useful power. The selection is performed in each OFDM symbol, independently. We identify this strategy as Instantaneous Energy Selection (IES). Firstly, we sort the vector of CIR estimate samples in descending order of absolute values:

$$|\hat{h}_{i(0),\ell}|\geq|\hat{h}_{i(1),\ell}|\geq\ldots\geq|\hat{h}_{i(j),\ell}|\geq\ldots\geq|\hat{h}_{i(N_p-1),\ell}| \tag{48}$$

where $i(j)$ is an indexing function introduced to represent the sorting function applied to the CIR estimates samples, in descending order. Then, we keep accumulating the MSS as long as the total energy remains below the target T:

$$\mathcal{S}_{\mathrm{IES}}(\ell)\equiv\left\{i(j):\sum_{v=0}^{j-1}|\hat{h}_{i(v),\ell}|^2\leq T,\ j=0,\ldots,N_p-1\right\} \tag{49}$$

The target T corresponds to the estimate of the total received useful power:

$$T=\sum_{i=0}^{N_p-1}|\hat{h}_i|^2-\sum_{i=0}^{N_p-1}E[|\nu_i|^2]=\sum_{i=0}^{N_p-1}|\hat{h}_i|^2-\frac{1}{\rho} \tag{50}$$

B. Average Energy Selection

All selection strategies described so far were pointing at finding $S_{opt}(\ell)$. Unfortunately, their instantaneous nature makes them vulnerable to noise sparks which are erroneously reckoned as channel taps. As an alternative, it may be more efficient to point at S_{avg} by extending the observation window over several OFDM symbols, which allows filtering. As a consequence, higher reliability of the MSS selection and therefore better estimation performance are expected, especially in low SNR conditions. In particular, we select as MSSs those samples whose CIR estimate sample energy, measured in an observation window of W OFDM symbols, overcomes a threshold, ζ:

$$\mathcal{S}_{\mathrm{AES}}(\ell)\equiv\left\{i:\hat{E}_{i,\ell}>\zeta,\ i=0,\ldots,N_p-1\right\} \tag{51}$$

where:

$$\hat{E}_{i,\ell}=\frac{1}{W}\sum_{v=\ell-W+1}^{\ell}|\hat{h}_{i,v}|^2 \tag{52}$$

The observation window length, W, is an important parameter upon which estimation performance is strongly dependent. In the case of wide-sense stationary channels, the larger W the more accurate the energy estimation, but this increases latency and required memory at the receiver. Also, in the case of non-stationary channels, it is necessary to limit W in order to track time varying channel statistics.

We derive the noise and tap holding probabilities. Since for $i\notin\mathcal{C}$ the samples $\hat{h}_{i,\ell}$ are mutually statistically independent complex Gaussian variables, with zero mean and variance $(2\rho N_p)^{-1}$ per branch, P^{NH} for AES with observation window length W and threshold ζ is given by:

$$P^{\mathrm{NH}}=\mathrm{Prob}\left[\hat{E}_{i,\ell}>\zeta\middle|\, i\notin\mathcal{C}\right]= \tag{53}$$
$$=\mathrm{e}^{-W\rho N_p\zeta}\sum_{v=0}^{W-1}\frac{(W\rho N_p\zeta)^v}{v!}\quad\forall i\notin\mathcal{C} \tag{54}$$

The analytical derivation is provided in Appendix B.

On the other hand, considering the case $i\in\mathcal{C}$, the samples $\hat{h}_{i,\ell}$ are statistically correlated. In particular, time correlation depends on the ratio between the channel coherence time, which depends on the terminal speed, and the OFDM symbol duration. In the following, we analyze two extreme cases, considering a very rapid and very slow channel respectively. In the first case, we assume that the Doppler spread is large enough to break the time correlation of the CIR estimate

samples, belonging to different received OFDM symbols[5]. The corresponding $\hat{h}_{i,\ell}$ samples in successive OFDM symbols result to be mutually statistically independent complex Gaussian variables, with zero mean and branch variance $\gamma_i^2/2 + (2\rho N_p)^{-1}$. Consequently, the TH probability is given by:

$$P_i^{\text{TH}} = \text{Prob}\left[\hat{E}_{i,\ell} > \zeta \,|\, i \in \mathcal{C}\right] = \\ = \mathrm{e}^{-\frac{W\rho N_p \zeta}{1+\gamma_i^2 \rho N_p}} \sum_{v=0}^{W-1} \frac{1}{v!} \left(\frac{W\rho N_p \zeta}{1+\gamma_i^2 \rho N_p}\right)^v \quad \forall\, i \in \mathcal{C} \quad (55)$$

In the second case, we assume that the Doppler spread is small enough to guarantee a quasi-static channel within the observation window length; therefore, the CIR sample estimates, $\hat{h}_{i,\ell}$, can be seen as the sum of a static channel complex coefficient [6] $\tilde{h}_i = h_{i,\ell}$, and noise. The corresponding $\hat{h}_{i,\ell}$ in successive OFDM symbols are again mutually statistically independent complex Gaussian variables (because noise is white), with mean $\tilde{h}_i$ and variance per branch $(\rho N_p)^{-1}$. In this case, $\hat{E}_i$ is distributed as a non-central chi-square distribution with non-centrality parameter $\lambda_i = |\tilde{h}_i|^2$. The corresponding TH probability is given by:

$$P_i^{\text{TH}} = \text{Prob}\left[\hat{E}_{i,\ell} > \zeta\right] = 1 - \frac{(\rho N_p)^W}{\gamma_i^2 \Gamma(W)} \\ \int_0^{\zeta} \int_0^{\infty} x^{W-1} \mathrm{e}^{-(\lambda_i \gamma_i^2 + \rho N_p (x + W\lambda_i))} \\ {}_0F_1\left(W; (\rho N_p)^2 W \lambda_i x\right)\, d\lambda_i\, dx \quad (56)$$

The analytical derivation is provided in Appendix B.

Similarly to the TCS case, the appropriate ζ setting depends on channel statistics, as well as on W. Since the analytical derivation of the optimal threshold ζ in this case is unfeasible, due to the fact that several integral forms are involved, we propose an alternative strategy which, as we show in the following, achieves performance very close to the $\text{MSE}(avg)$ lower bound. Assuming that W is large enough to eliminate noise holding events, we can set the threshold ζ according to the definition $\mathcal{S}_{avg}$, here re-written in terms of E_i:

$$i \in \mathcal{S}_{avg} \Longleftrightarrow E_i > \frac{2}{N_p \rho} = \zeta \quad (57)$$

Substituting (57) into (53), we obtain a very simple and intuitive expression:

$$P^{\text{NH}} = \mathrm{e}^{-2W} \sum_{v=0}^{W-1} \frac{(2W)^v}{v!} \quad (58)$$

It is interesting to note that, in this case, the noise holding probability depends only on the observation window length. The performance of this method is very good for large W, as can be expected, while it reduces to TCS for $W = 1$, in which case other threshold setting strategies are more appropriate.

VI. Numerical Results and Discussion

The purpose of this Section is twofold: first, we assess pure channel estimation performance in terms of MSE and validate our analytical models; second, we evaluate the impact of using the proposed channel estimators in terms of BER at the output of the channel decoder. In order to have practically significant results, we consider the standardized coded OFDM system, DVB-SH [17]. DVB-SH foresees the 3GPP2 turbo code and a convolutional interleaver. In order to set the system dynamics, we assume that the DVB-SH system is operating in S-band (2 GHz) with 5 MHz of bandwidth, and the terminal speed is 50 km/h. We used Monte Carlo simulations to evaluate both MSE and BER. Two different channel models are used: a 6-taps uniform channel and the ITU-TU6 channel, the power delay profiles of which are reported in Table I. As outlined in Section II, in the analysis we have assumed a uniformly scattered pilot pattern over the entire frequency comb, which, as shown in [12], is the best pilot arrangement in terms of channel estimation MMSE. However, DVB-SH, as well as other standards, does not provide a perfectly uniform scattered pilot pattern because of the insertion of guardbands. In fact this standard uses $N = 1024$ carriers, with $N_p = 71$ scattered pilots distributed over the first $N_a = 852$ active subcarriers. As a consequence, the resulting pilot pattern is not optimal in terms of MSE, and the CIR taps become correlated [8]. To the end of assessing the impact on the performance of our proposed algorithms we also report simulation results in the presence of CIR correlation.

TABLE I
NORMALIZED POWER DELAY PROFILE OF THE CONSIDERED MULTIPATH CHANNELS

	Taps	#1	#2	#3	#4	#5	#6
Uniform Channel	Delay[μs]	0.0	1.05	2.1	3.15	4.2	5.25
	Power[dB]	-7.78	-7.78	-7.78	-7.78	-7.78	-7.78
ITU TU6	Delay[μs]	0.0	0.2	0.5	1.6	2.3	5.0
	Power[dB]	-7.22	-4.22	-6.22	-10.22	-12.22	-14.22

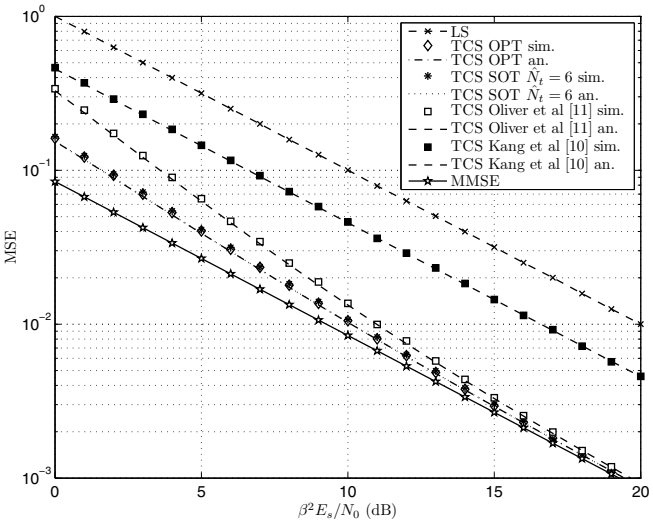

Fig. 3. Comparison between analytical, obtained from eq. (41), and simulated performance of several TCS selection strategies with uniform channel with $N_t = 6$.

A. MSE performance

Our intent here is first to validate our analytical models through numerical results obtained by simulation and second

[5]Since we assumed that $h_j(t)$ is constant over a single OFDM symbol, this corresponds to a block fading channel model.

[6]here we can drop the index ℓ because in quasi-static channel the channel taps are assumed to be constant over the entire observation windows

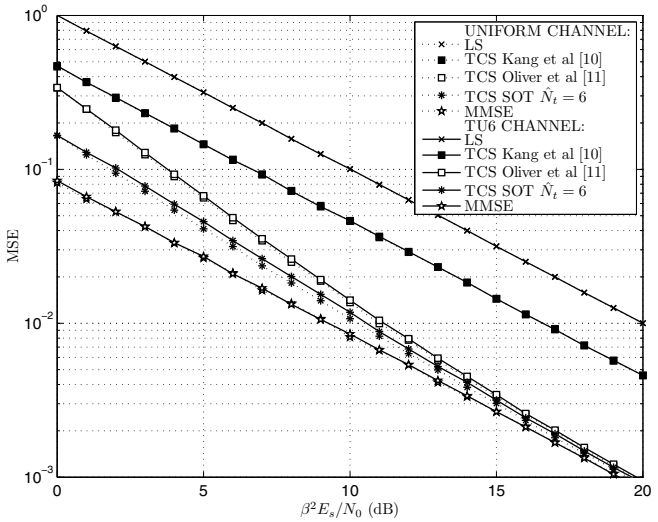

Fig. 4. Comparison between the performance of several threshold based MSS selection strategies with TU6 and uniform channel.

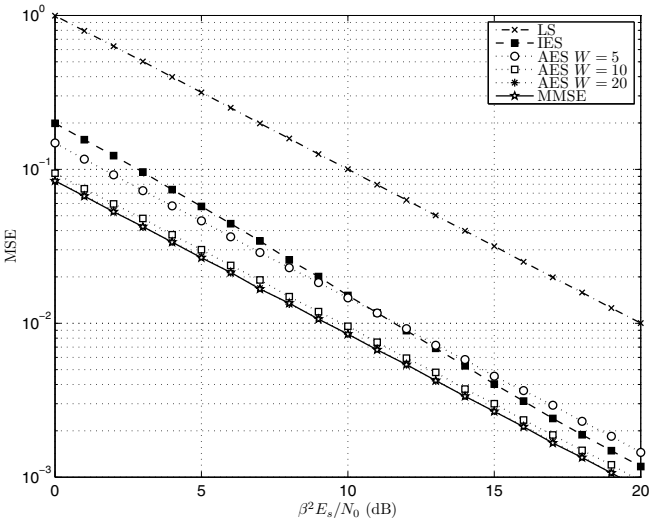

Fig. 6. Comparison between the proposed MMS selection strategies based on energy estimation, using TU6, 50 km/h.

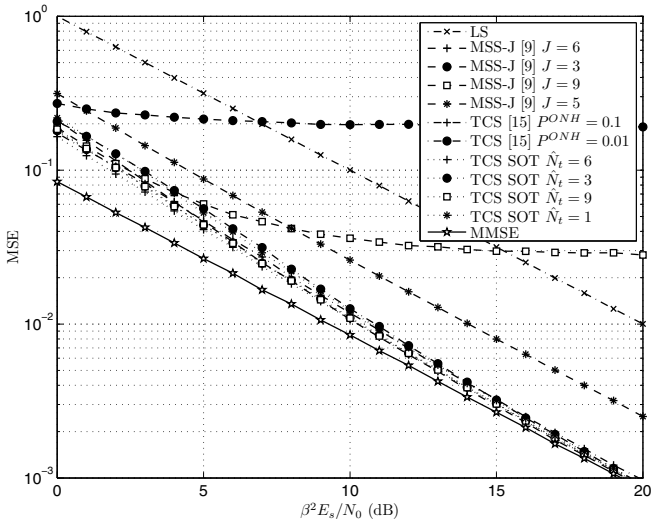

Fig. 5. Comparison between TCS with Sub-Optimal threshold, TCS [15], and the method proposed in [9] using TU6 channel ($N_t = 6$). Different mismatch levels between the actual and the assumed number of taps.

to assess the performance and robustness of the proposed MSS algorithms against channels with different power delay profiles, and non-uniform pilot pattern.

In Fig. 3, we report the results for the proposed TCS algorithms (with optimal and sub-optimal thresholds) and for the state-of-art alternatives over the uniform channel using a uniformly scattered pilot patterns. We observe that the $\mathrm{MSE}^{\mathrm{TCS}}$ computed with (41) and the appropriate threshold value, is in perfect agreement with the numerical performance of all TCS algorithms. Comparing TCS methods, SOT reaches the best results among the practical algorithms, and is also very close to the optimum threshold results. At MSE $= 10^{-2}$ the gain is larger than 10 dB and 6 dB with respect to the LS and TCS [10] methods, respectively. Even the criterion proposed in [11], which takes advantage of the KCS, is outperformed by SOT. Moreover, SOT is also close to MMSE at high SNR.

Clearly the uniform channel is the best match for our SOT strategy. Therefore, it is important to verify the performance in non-uniform channels. In Fig. 4, the numerical results using both uniform and ITU-TU6 channels are illustrated. It is important to note that the SOT performance for the ITU-TU6 channel is only slightly worse than the a uniform channel case. Furthermore, comparing TCS methods, SOT has the best performance for both considered channels, and for high SNR it approaches MMSE.

In Fig. 5, we report the comparison between SOT and the MSS-J selection strategy proposed in [9] using the ITU-TU6 channel and uniform pilot pattern. Since both methods require the knowledge of the number of the channel taps, N_t, we tested the robustness to a mismatch on this parameter. Even in the case of no mismatch, SOT outperforms MSS-J. When J differs from N_t, MSS-J performance degrades rapidly. On the other hand, SOT has good performance even in the case of a large mismatch. Furthermore, in Fig. 5, we also report the comparison between SOT and TCS proposed in [15] considering two indicated values of the parameter P^{ONH}. SOT outperforms TCS proposed in [15], even in the case of a mismatch.

Fig. 6 shows the numerical results considering the ITU-TU6 channel, for the proposed IES and AES strategies. Regarding the AES method, the threshold ζ has been set according to (57). Numerical results show that, by using an observation window equal or greater than 10 OFDM symbols ($W \geq 10$), AES approaches very closely MMSE outperforming all other considered methods (not reported in this Figure). Even in the case of $W = 5$, AES outperforms the other selection strategies in the low SNR region. Using smaller W, AES performance degrades.

As discussed before, it is necessary to verify the estimation performance of the proposed algorithms when the condition of uncorrelated CIR taps is violated. In Figs. 7 and 8, we compare the proposed schemes (SOT, IES and AES) with the state-

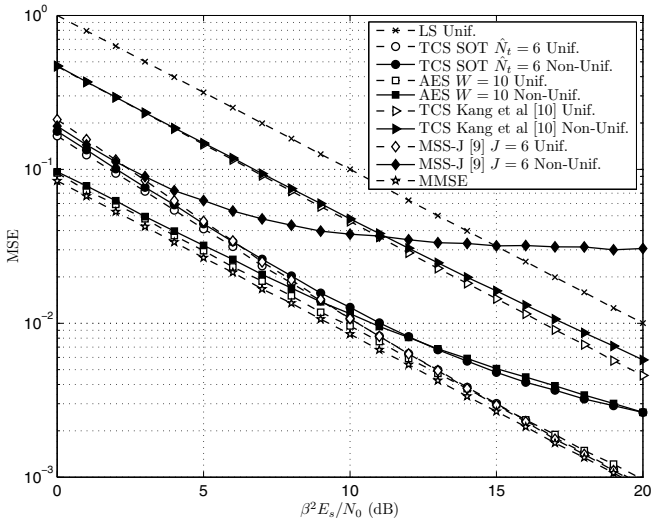

Fig. 7. Channel estimation performance of the proposed algorithms, SOT and AES with $W = 10$, compared with the state-of-art alternatives, considering both the cases of uniform and non-uniform pilot pattern with the same number of pilots, $N_p = 71$.

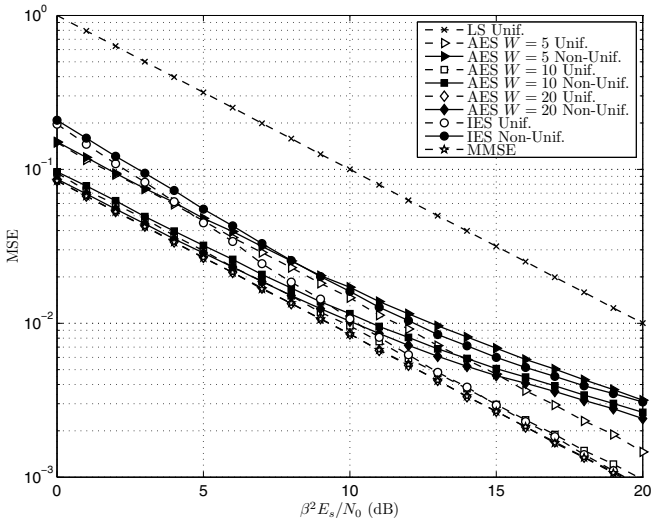

Fig. 8. Channel estimation performance of the proposed algorithms, IES and AES with several values of W, considering both the cases of uniform and non-uniform pilot pattern with the same number of pilots, $N_p = 71$.

of-art alternatives using both uniform and non-uniform pilot patterns (as standardized by DVB-SH), with the same number of pilots, $N_p = 71$. As a consequence of correlation among CIR estimates, MSE performance deteriorates with respect to uniform pilot pattern case. Nevertheless, the proposed SOT and AES with $W \geq 10$ are still the best solutions among the practical channel estimation methods.

Summarizing, numerical results show that AES with $W \geq 10$ outperforms all other methods, especially in the low SNR region, closely approaching MMSE. This holds true even when the condition of uncorrelated CIR estimated samples is not verified, due to non-uniform pilot pattern. On the other hand, SOT is a strong alternative, especially in the high SNR region, considering its lower latency. Concerning the IES strategy, numerical results show that this method achieves good performance, even if it is outperformed by SOT and AES.

B. BER performance

Here we consider the impact of using different channel estimation methods on the DVB-SH BER. In Figs. 9 and 10, we report BER for QPSK modulation and turbo code rate 1/4 and 1/2 respectively, and in Fig. 11 we report BER for 16QAM modulation and turbo code rate 1/2. we consider TU6 channel and with terminal speed equal to 50 km/h. In order to make a complete comparison we present the results for both uniform and non-uniform pilot patterns. In the uniform pilot pattern case, the numerical results confirm the trend observed in MSE performance assessments: BER using AES is very close to the case of using MMSE channel estimation for all the considered modulations and coding rates. Using SOT for QPSK and coding rate 1/4, we observe performance gaps of 0.5 dB with respect to MMSE, and 1 dB with respect to ideal channel estimation. These gaps become smaller when using QPSK and 16QAM with coding rate 1/2. In particular,

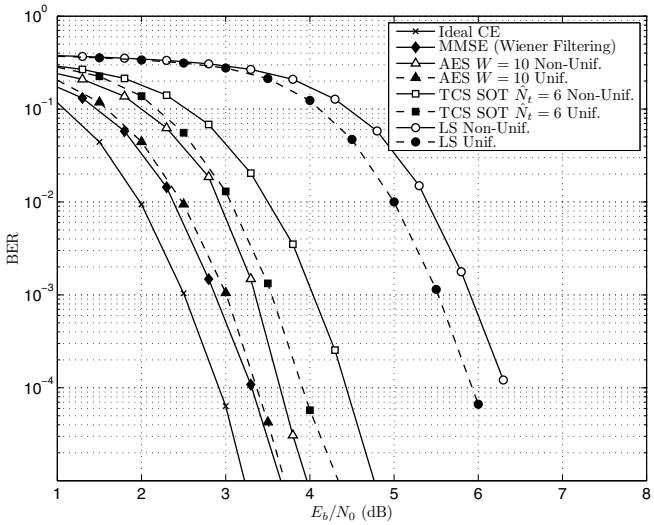

Fig. 9. Coded DVB-SH BER performance, QPSK,turbo code rate 1/4, considering both the cases of uniform and non-uniform pilot pattern with the same number of pilots, TU6, 50 km/h.

considering 16QAM, both AES and SOT methods converge to the MMSE case, and are close to ideal channel estimation performance.

In the non-uniform pilot pattern case, a BER increase can be observed performance decreases because of the correlation between CIR taps. In particular, with respect to Wiener Filtering case at $\mathrm{BER} = 10^{-3}$ we observe performance gaps of: 0.3 dB for AES, and 1 dB for SOT, using QPSK and coding rate 1/4; 0.9 dB for AES, and 1.4 dB for SOT, using QPSK and coding rate 1/2; and finally, 2 dB for AES, and of 2.4 dB for SOT, using 16QAM and coding rate 1/2.

Summarizing, comparing the ideal and real channel estimation cases, using a uniform pilot pattern, the performance loss due to the estimation error is smaller for higher modulation order and coding rate. In fact, in this case, the SNR working

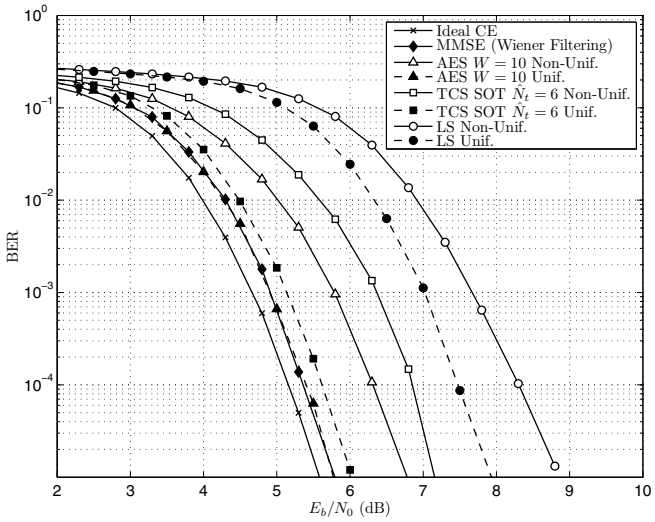

Fig. 10. Coded DVB-SH BER performance, QPSK,turbo code rate 1/2, considering both the cases of uniform and non-uniform pilot pattern with the same number of pilots, using TU6 , 50 km/h.

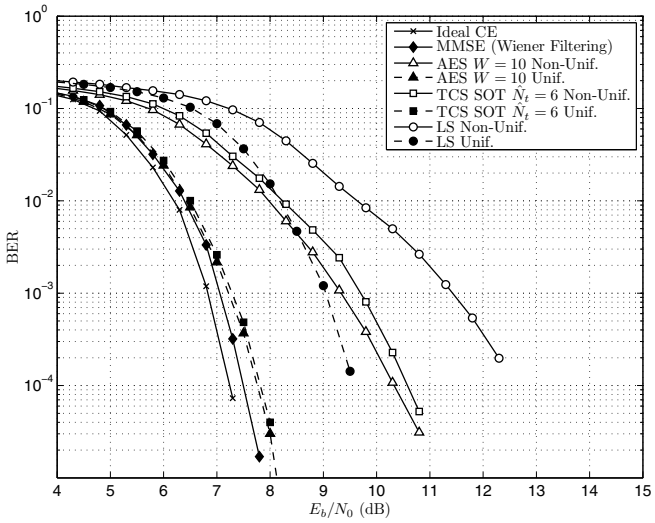

Fig. 11. Coded DVB-SH BER performance, 16QAM, turbo code rate 1/2, considering both the cases of uniform and non-uniform pilot pattern with the same number of pilots, using TU6, 50 km/h.

point is higher, thus the channel estimation MSE lowers. On the other hand, using a non-uniform pilot pattern, the performance loss is greater for higher modulation order and coding rate. In fact, in this case, the required channel estimation quality is higher but as a consequence of the MSE error floor due to the CIR estimates correlation, channel estimation MSE is bounded.

In conclusion, numerical results confirm that the proposed algorithms based on MSS selection of the CIR estimate guarantee a significant gain even in those practical cases where correlation among CIR estimate samples occurs. Moreover, using lower modulation order and coding rate, the proposed algorithms approach the MMSE case in terms of BER performance.

VII. Conclusions

In this paper, we have addressed the problem of OFDM data-aided channel estimation, giving emphasis on the fact that KCS is hardly available at the receiver; therefore the MMSE approach is hardly applicable in practice. Our aim has been to improve over LS channel estimation by selecting the MSSs of the CIR, achieving good MSE performance, while avoiding the need for a-priori KCS. Starting from the definition of the optimal set of samples in the instantaneous and average senses, we derived lower bounds on the estimation MSE for any MSS selection strategy, showing that the MSS approach has the potential to reach the optimum MMSE performance. We have considered three practical MSS selection strategies: TCS and IES which pursue instantaneous decimation, and AES which is oriented towards windowed selection. Regarding TCS, we have provided a novel analytical characterization, through which we derived the closed form for the MSE, and consequently, the optimum threshold in the minimum MSE sense and a sub-optimal but practical version. Numerical results confirm that these three novel solutions (SOT, IES, AES) outperform previous methods, for both uncorrelated and correlated CIR samples, with AES being the best when the observation window size is sufficiently large.

Appendix A
MSE using $S_{opt}(\ell)$

Let's consider the Rayleigh random variables $\alpha_{h_i} = |h_{i,\ell}|$ and $\alpha_{\nu_i} = |\nu_{i,\ell}|$. The MSE achievable by using the optimum set of samples $S_{opt}(\ell)$, after considerable algebra, can be expressed by:

$$\begin{aligned}&\mathrm{MSE}(opt) = E\left[\mathrm{SE}_{min}(\ell)\right] = \\ &= \sum_{i\in\mathcal{C}} \left\{ \int_0^{\infty} \left(\int_0^{\alpha_{\nu_i}} \alpha_{h_i}^2 p_{\alpha_{h_i}}(\alpha_{h_i})\, d\alpha_{h_i} \right) p_{\alpha_{\nu_i}}(\alpha_{\nu_i})\, d\alpha_{\nu_i} + \right. \\ &\left. + \int_0^{\infty} \left(\int_0^{\alpha_{h_i}} \alpha_{\nu_i}^2 p_{\alpha_{\nu_i}}(\alpha_{\nu_i})\, d\alpha_{\nu_i} \right) p_{\alpha_{h_i}}(\alpha_{h_i})\, d\alpha_{h_i} \right\} \quad (59)\end{aligned}$$

where the corresponding p.d.f. of which are given by:

$$p_{\alpha_{h_i}}(\alpha_{h_i}) = \frac{2\alpha_{h_i}}{\gamma_i^2} \mathrm{e}^{-\frac{\alpha_{h_i}^2}{\gamma_i^2}} \quad (60)$$

$$p_{\alpha_{\nu_i}}(\alpha_{\nu_i}) = 2\rho N_p \alpha_{\nu_i} \mathrm{e}^{-\rho N_p \alpha_{\nu_i}^2} \quad (61)$$

Substituting (60) and (61) in (59), and, after considerable algebra, it can be found that:

$$\begin{aligned}\mathrm{MSE}(opt) &= \sum_{i\in\mathcal{C}} \left[\frac{\gamma_i^2}{(1+\gamma_i^2\rho N_p)^2} + \frac{\gamma_i^4 \rho N_p}{(1+\gamma_i^2\rho N_p)^2} \right] = x \\ &= \sum_{i\in\mathcal{C}} \frac{\gamma_i^2}{1+\rho N_p \gamma_i^2} \quad (62)\end{aligned}$$

Appendix B
Tap and Noise Holding Probabilities

Let's consider the vector $\mathbf{h}_i = \{h_{i,\ell-W+1}, h_{i,\ell-W+2}, \ldots, h_{i,\ell}\}$ containing the W complex Gaussian random variables representing the complex tap gains at the ℓ-th OFDM symbol for a given delay i. According to

the Rayleigh fading assumption, vector $\mathbf{h}_i$ can be modelled as a W-variate zero mean complex Gaussian variable with covariance matrix Σ, i.e. $\mathbf{h}_i \sim \mathcal{N}_{cW}(0, \Sigma)$. The measured CIR sample energy $\hat{E}_{i,\ell}$ reported in (52), conditioned on $\mathbf{h}_i$, can be modelled as a non-central chi-square distribution, $\chi^2_{2W}(\lambda)$, with $2W$ degrees of freedom, non-centrality parameter $\lambda = \frac{1}{W}\sum_{v=\ell-W+1}^{\ell} |h_{i,v}|^2$, and $\sigma^2 = (2\rho N_p W)^{-1}$,

$$p_{\hat{E}_{i,\ell}|\mathbf{h}_i}(x|\mathbf{h}_i) = \frac{x^{W-1}}{(2\sigma^2)^W \Gamma(W)} \mathrm{e}^{-\frac{x+\lambda}{2\sigma^2}} {}_0F_1\left(W; \frac{\lambda x}{(2\sigma^2)^2}\right) \tag{63}$$

where $\Gamma(W) = (W-1)!$ and ${}_0F_1(b;z)$ is a particular case of the generalized hypergeometric function ${}_mF_n(a_1, \ldots a_m; b_1, \ldots b_n; z)$ [18]. We start from the non-central chi-square definition based on the hypergeometric function in order to treat in the following the central chi-square as a particular case of non-central case [19, Appendix I].

A. Noise Holding Case: $i \notin \mathcal{C}$

Let's consider the case where $i \notin \mathcal{C}$. In this case $\mathbf{h}_i = \bar{0}$ with probability 1, and consequently $\lambda = 0$. Therefore, $\hat{E}_{i,\ell}$ can be modelled as a central chi-square random variable $\chi^2_{2W}(0)$ with $\sigma^2 = (2\rho N_p W)^{-1}$:

$$p_{\hat{E}_{i,\ell}}(x) = \frac{x^{W-1}(\rho N_p W)^W}{\Gamma(W)} \mathrm{e}^{-x\rho N_p W} \qquad \forall i \notin \mathcal{C} \tag{64}$$

Thus P^{NH} is given by:

$$\begin{aligned} P^{\mathrm{NH}} =& \mathrm{Prob}\left[\hat{E}_{i,\ell} > \zeta \middle| i \notin \mathcal{C}\right] = \\ =& \mathrm{e}^{-W\rho N_p \zeta} \sum_{v=0}^{W-1} \frac{(W\rho N_p \zeta)^v}{v!} \qquad \forall i \notin \mathcal{C} \end{aligned} \tag{65}$$

Setting ζ according to (57), it follows:

$$P^{\mathrm{NH}} = \mathrm{e}^{-2W} \sum_{v=0}^{W-1} \frac{(2W)^v}{v!} \qquad \forall i \notin \mathcal{C} \tag{66}$$

B. Tap Holding with Uncorrelated Fading: $i \in \mathcal{C}$ and $\Sigma = Diag(\gamma_i^2)$

Let's consider the particular case where $i \in \mathcal{C}$, and the elements of $\mathbf{h}_i$ are zero-mean complex Gaussian variables i.i.d. with variance γ_i^2 (i.e. the covariance matrix Σ is diagonal). In this case $\hat{E}_{i,\ell}$ can be modelled as a central chi-square random variable $\chi^2_{2W}(0)$ with $\sigma^2 = (\gamma_i^2/2 + 1/(2\rho N_p))/W$. Therefore, similarly to the previous case, P_i^{TH} is given by:

$$\begin{aligned} P_i^{\mathrm{TH}} =& \mathrm{Prob}\left[\hat{E}_{i,\ell} > \zeta \,\middle|\, i \in \mathcal{C}\right] = \\ =& \mathrm{e}^{-\frac{W\rho N_p \zeta}{1+\gamma_i^2 \rho N_p}} \sum_{v=0}^{W-1} \frac{1}{v!} \left(\frac{W\rho N_p \zeta}{1+\gamma_i^2 \rho N_p}\right)^v \qquad \forall\, i \in \mathcal{C} \end{aligned} \tag{67}$$

C. Tap Holding with Perfectly Correlated Fading: $i \in \mathcal{C}$ and $\mathbf{h}_i = \tilde{h}_i$

Let's consider the particular case where $i \in \mathcal{C}$, and all the elements of $\mathbf{h}_i$ are equal to $\tilde{h}_i$. In this case, $\hat{E}_{i,\ell}$ can be modelled as a non-central $\chi^2_{2W}(\lambda_i)$, with non-centrality parameter $\lambda_i = |\tilde{h}_i|^2$, and $\sigma^2 = (2\rho N_p W)^{-1}$:

$$\begin{aligned} p_{\hat{E}_{i,\ell}}(x|\lambda_i) = \frac{x^{W-1}(\rho N_p W)^W}{\Gamma(W)} \mathrm{e}^{-\rho N_p W^2 (x+\lambda_i)} \\ {}_0F_1\left(W; (\rho N_p W)^2 \lambda_i x\right) \end{aligned} \tag{68}$$

The non-centrality parameter λ_i is itself distributed as a $\chi^2_2(0)$ with branch variance equal to $\gamma_i^2/2$. After removing the conditioning on λ_i the tap holding probability is given by:

$$\begin{aligned} P_i^{\mathrm{TH}} = \frac{2(\rho N_p W)^W}{\gamma_i^2 \Gamma(W)} \int_{\zeta}^{\infty} \int_0^{\infty} \lambda_i x^{W-1} \mathrm{e}^{-(\lambda_i/\gamma_i^2 + \rho N_p W(x+\lambda_i))} \\ {}_0F_1\left(W; (\rho N_p W)^2 \lambda_i x\right)\, d\lambda_i\, dx \quad \forall\, i \in \mathcal{C} \end{aligned} \tag{69}$$

REFERENCES

[1] L. J. Cimini, Jr., "Analysis and simulation of a digital mobile channel using orthogonal frequency division multiplexing," *IEEE Trans. Commun.*, vol. COM-33, pp. 665–675, July 1985.

[2] J. A. C. Bingham, "Multicarrier modulation for data transmission: an idea whose time has come," *IEEE Commun. Mag.*, vol. 28, no. 5, pp. 5–14, 1990.

[3] P. Hoeher, S. Kaiser, and P. Robertson, "Two-dimensional pilot symbol aided channel estimation by Wiener filtering," in *Proc. 1997 IEEE International Conf. Acoustics, Speech Signal Process.*, vol 3, pp. 1845–1848.

[4] P. Hoeher, S. Kaiser, and P. Robertson, "Pilot-symbol-aided channel estimation in time and frequency," in *1997 Proc. Commun. Theory Mini-Conf. within IEEE Global Telecommun. Conf.*, pp. 90–96, 1997.

[5] Y. Li, L. J. Cimini Jr., and N. R. Sollenberger, "Robust channel estimation for OFDM systems with rapid dispersive fading channels," *IEEE Trans. Commun.*, vol. 46, no. 7, pp. 902–915, July 1998.

[6] O. Edfors, M. Sandell, J. J. van de Beek, S. K. Wilson, and P. O. Borjesson, "OFDM channel estimation by singular value decomposition," *IEEE Trans. Commun.*, vol. 46, no. 7, pp. 931–939, July 1998.

[7] O. Edfors, M. Sandell, J. J. van de Beek, S. K. Wilson, and P. O. Borjesson, "Analysis of DFT-based channel estimators for OFDM," *Wireless Personal Commun.: An International J.*, vol. 12 no. 1, p. 55–70, Jan. 2000.

[8] M. Morelli and U. Mengali, "A comparison of pilot-aided channel estimation methods for OFDM systems," *IEEE Trans. Signal Process.*, vol. 49, no. 2, pp. 3065–3073, Dec. 2001.

[9] H. Minn and V. K. Bhargava, "An investigation into time-domain approach for OFDM channel estimation," *IEEE Trans. Broadcast.*, vol. 46, no. 4, pp. 240–248, Dec. 2000.

[10] Y. Kang, K. Kim, and H. Park, "Efficient DFT-based channel estimation for OFDM systems on multipath channels," *IET Commun.*, vol. 1, no. 2, pp. 197–202, Apr. 2007.

[11] J. Oliver, R. Aravind, and K. M. M. Prabhu, "Sparse channel estimation in OFDM systems by threshold-based pruning," *Electron. Lett.*, vol. 44, no. 13, pp. 830–832, June 2008.

[12] R. Negi and J. Cioffi, "Pilot tone selection for channel estimation in a mobile OFDM system," *IEEE Trans. Consumer Electron.*, vol. 44, no. 3, pp. 1122–1128, Aug. 1998.

[13] D. Tse and P. Viswanath, *Fundamentals of Wireless Communication*. Cambridge University Press, 2005.

[14] M. Speth, S. A. Fechetl, G. Fock, and H. Meyr, "Optimum receiver design for wireless broad-band system using OFDM—part I," *IEEE Trans. Commun.*, vol. 47, no. 11, pp. 571–578, Nov. 1999.

[15] S. Rosati, G. E. Corazza, and A. Vanelli-Coralli, "OFDM channel estimation with optimal threshold-based selection of CIR samples," in *Proc. 2009 IEEE Global Telecommun. Conf.*, pp. 1–7.

[16] S. Rosati, A. B. Awoseyila, A. Vanelli-Coralli, C. Kasparis, G. E. Corazza, and B. G. Evans, "Threshold detection analysis for OFDM timing and frequency recovery," in *Proc. 2009 IEEE Global Telecommun. Conf.*, pp. 1–5.

[17] , "Digital video broadcasting (DVB); framing structure, channel coding and modulation for satellite transmission to handheld (DVB-SH)," ETSI EN 302 583 V1.0.0, June 2007.

[18] M. Abramowitz and I. A. Stegun, *Handbook of Mathematical Functions*. Dover, 1970.

[19] G. E. Corazza and R. De Gaudenzi, "Analysis of coded noncoherent transmission in DS-CDMA mobile satellite communications," *IEEE Trans. Commun.*, vol. 46, no. 11, pp. 1525–1535, Nov. 1998.

Stefano Rosati is a Post-Doc Research Engineer at the École Polytechnique Fédérale de Lausanne (EPFL), (Switzerland). He received the Dr. Ing. Degree (summa cum laude) in Electronics and Telecommunication Engineering and the Ph.D. in Electronics and Computer Science and Telecommunications from the University of Bologna (Italy) in 2007 and 2011, respectively. From 2007 to 2011, he has also been with the Advanced Research Center for Electronic Systems (ARCES) of the University of Bologna. During this period he was actively involved in the next generation mobile digital broadcasting standardization. In 2010, he was an Intern Engineer at Corporate R&D Department of Qualcomm Inc. (San Diego, CA), working on Mobile Communication Systems. In 2011 he joined the Information Processing Group (IPG) and the Mobile Communications Laboratory (LCM) of the EPFL, (Switzerland). His research activities are mainly focused on next-generation cellular communication systems, and terrestrial and satellite broadcast networks. In particular, his interests are in OFDM synchronization techniques, OFDM channel estimation, PAPR Reduction and enhanced MIMO techniques. He has authored several scientific papers and internationals patents regarding these topics.

Giovanni Emanuele Corazza is a Full Professor at the University of Bologna, Head of the Department of Electronics, Computer Science and Systems (DEIS), and founder of the Marconi Institute for Creativity (2011). He was Chairman of the School for Telecommunications in the years 2000-2003, Chairman of the Advanced Satellite Mobile Systems Task Force (ASMSTF), Founder and Chairman of the Integral Satcom Initiative (ISI), a European Technology Platform devote to Satellite Communications. In the years 1997-2012, he has served as Editor for Communication Theory and Spread Spectrum for the IEEE TRANSACTIONS ON COMMUNICATIONS. He is author of more than 200 papers, and received the Marconi International Fellowship Young Scientist Award in 1995, the IEEE 2009 Satellite Communications Distinguished Service Award, the 2002 IEEE VTS Best System Paper Award, the Best Paper Award at IEEE ISSSTA98, at IEEE ICT2001, and at ISWCS 2005. He has been the General Chairman of the IEEE ISSSTA 2008, ASMS 2004, ASMS 2006, ASMS 2008, ASMS 2010 Conferences. His research interests are in wireless and satellite communications, estimation and synchronization, spread spectrum and multi-carrier transmission, upper layer coding, navigation and positioning, scientific creative thinking.

Alessandro Vanelli-Coralli received the Dr. Ing. Degree (cum laude) in Electronics Engineering and the Ph.D. in Electronics and Computer Science from the University of Bologna (Italy) in 1991 and 1996, respectively. In 1996, he joined the Department of Electronics, Computer Science and Systems (D.E.I.S.) at the University of Bologna, where he is currently an Associate Professor. Since 2001, he has also been with the Advanced Research Center for Electronic Systems (ARCES) of the University of Bologna. During 2003 and 2005, he was a Visiting Scientist at Qualcomm Inc. (San Diego, CA), working in the Corporate R&D Department on Mobile Communication Systems. Dr. Vanelli-Coralli participates in national and international research projects on satellite mobile communication systems. He is the Co-Leader of the R&D group of the Integral SatCom Initiative (ISI) technology platform, and Scientific Responsible for several European Space Agency and European Commission funded projects. His research interests are in the area of wireless communication systems, digital transmission techniques, and digital signal processing. Dr. Vanelli-Coralli has been appointed member of the Editorial Board of the *Wiley InterScience Journal on Satellite Communications and Networks* and has been guest co-Editor for several special issues in of international scientific journals. Dr. Vanelli-Coralli has served in the organization committees of scientific conferences and Technical Chairman of the 4th IEEE ASMS 2008 Conference and Technical Vice-Chairman of the IEEE ISSSTA 2008 Conference. In 2010 and 2012 has served as General Co-Chairman of the 5th and 6th IEEE ASMS Conference. Dr. Vanelli-Coralli co-authored more than 130 papers and scientific conference contributions and he is co-recipient of several Best Paper Awards. He is an IEEE Senior Member.